Cite this: DOI: 10.1039/xxxxxxxxxx

Black-CuO: Surface-enhanced Raman scattering and infrared properties

Armandas Balčytis,[*a,b] Meguya Ryu,[c] Gediminas Seniutinas,[a] Jurga Juodkazytė,[b] Bruce C. C. Cowie,[d] Paul R. Stoddart,[a] Massimiliano Zamengo,[c] Junko Morikawa[c] and Saulius Juodkazis[a,e]

Large surface area samples of nanotextured black CuO were prepared by chemical etching of Cu for use in surface-enhanced Raman scattering (SERS). The SERS intensity of a self-assembled monolayer (SAM) of thiophenol was proportional to the thickness of a nanoscale-conformal Au film deposited by magnetron sputtering over the black CuO. A very high SERS yield of $\sim 10^4$ counts·s^{-1}mW^{-1} was observed for the thiophenol SAM on the thickest Au films studied here. Synchrotron X-ray photoelectron spectroscopy was used to confirm that the surface of the chemically etched Cu was covered by high purity CuO. IR spectral characterization of the black CuO showed a close to linear increase in reflectivity from 25 to 100% over the range of 4000 - 500 cm^{-1} wavenumbers (or 2.5 - 20 μm in wavelength). Sensing applications and thermal effects in SERS are discussed.

Introduction

Nanotextured oxidised Cu (or black CuO) is a promising large surface area substrate for applications in surface-enhanced Raman scattering (SERS), catalysis, and microfluidics. Nano-sharp features of tens-of-nanometers in diameter are utilised in disparate fields, including anti-biofouling surfaces[1,2], bactericidal materials[3], and SERS substrates[4], as demonstrated by plasma-etched black-Si[5]. Since SERS has great potential for sensing applications in biomedical, forensic and security fields, the search for highly sensitive substrates (down to pico- or femto-molar concentrations) and practical fabrication methods has been vigorously pursued[6–8].

Surface-enhanced IR absorption spectroscopy (SEIRAS) is a complimentary technique for analytical finger printing of molecular species in gases or liquids. Recently it was demonstrated that simple metal mesh notch filters can be used to improve the sensitivity of SEIRAS detection of the potent greenhouse gas SF_6 down to ppm levels[9]. Direct enhancement of IR absorption by engineered plasmonic antennas was demonstrated for vibrational amide bands in silk[10]. The increased SEIRAS sensitivity is dependent on the creation of highly localised light intensity regions - hot spots - within the spectral transmission window of the notch filter[9] or resonant with the plasmonic antenna[10]. The utilisation of large surface area substrates on which notch filters or antennas are formed is a promising direction to further increase the sensitivity in SERS and SEIRAS. One of the simplest ways to increase the surface area by up to 10^2 times compared to the precursor metal surface is by chemical or anodic oxidation. Such oxidised surfaces are strongly light absorbing and scattering in the visible spectral range, but their performance in the IR has to be investigated further to find the optimum spectral range for the particular analyte molecules in SEIRAS. The heating due to light absorption on the black surface is another feature affecting SERS or SEIRAS and this effect needs a better understanding.

Black CuO surfaces produced by chemical oxidation of bulk Cu are among the oldest known spectrally selective photothermal absorbers, with low reflectance in the solar wavelength region (0.3 to 2.5 μm) and high reflectance in the infrared region (2.5 to 50 μm). The main drawback of these coatings is low resistance to thermal exposure[11,12]. CuO-based nanomaterials are of particular interest in the development of electrochemical biosensors. Recently, various nano-architectures of CuO have been explored for non-enzymatic glucose and hydrogen peroxide sensing[13–16]. Glucose concentration was measured with good accuracy and high precision in human serum[14].

Here, a study of the thermal diffusivity of black CuO in the IR spectral range is presented. Highly sensitive SERS performance of black-CuO is demonstrated and discussed with a view towards temperature-controlled adsorption/ desorption and chemical reactions on nano-textured black surfaces.

[a] *Faculty of Science, Engineering and Technology, Swinburne University of Technology, John Street, Hawthorn, VIC 3122, Australia. E-mail: abalcytis@swin.edu.au*
[b] *Center for Physical Sciences and Technology, A. Goštauto 9, LT-01108 Vilnius, Lithuania.*
[c] *Tokyo Institute of Technology, Meguro-ku, Tokyo 152-8550, Japan.*
[d] *Australian Synchrotron, 800 Blackburn Rd., Clayton, VIC 3168, Australia.*
[e] *Center for Nanotechnology, King Abdulaziz University, Jeddah 21589, Saudi Arabia.*

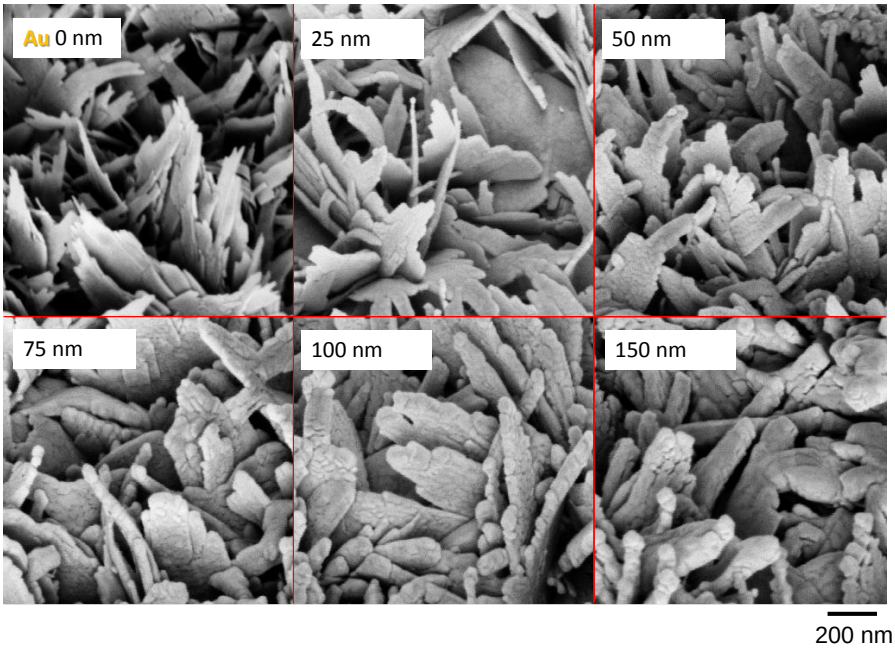

Fig. 1 Conformal coating: SEM images of black CuO with different thicknesses of sputtered Au, viewed from a 45°-tilt angle. Magnification = $30,000\times$. The indicated thicknesses are taken from the flat reference surface.

Experimental

Preparation of nanostructured cupric Cu(II) oxide (CuO) layers was performed by means of simple wet chemical etching of polished Cu foil in a 1.25M/66mM NaOH/$Na_2S_2O_8$ aqueous solution at 65 °C temperature over a duration of $t = 5$ min [17]. The surface area of the treated samples was up to 250 times larger than the initial flat Cu surface, as evaluated by cyclic voltammetry [18]. It by more than an order of magnitude exceeds the surface area of laser ablated sapphire used for SERS, measured using the same method [19], as well as that of black-Si [20].

The oxidation level and chemical bonding nature of the chemically nanostructured surface was investigated by X-ray photoelectron spectroscopy (XPS) conducted at the Soft X-ray spectroscopy beamline at the Australian Synchrotron. The capability to alter the X-ray photon energy was used to separate photoelectron and Auger electron contributions as well as to probe to different depths in the nanostructured material.

Infrared spectra were measured by Fourier transform (FTIR) spectrometry using a Spotlight 3000 (PerkinElmer) and attenuated total reflection (ATR) module on an Alpha-FTIR (Bruker) spectrometers.

The nanotextured CuO sufaces were magnetron sputtered with Au using an AXXIS physical vapor deposition (PVD) system (Kurt J. Lesker). Coating thickness was measured on a flat silica reference surface using a 3D optical profiler (Bruker). Due to the high surface area, the actual Au film thickness covering the CuO flakes was correspondingly thinner. Scanning electron microscopy (SEM) was carried out for structural inspection of the coatings (Raith 150TWO).

Raman scattering spectra were measured using an In-Via Raman microscope (Renishaw) with $\lambda = 785$ nm continuous wave laser excitation at $P = 690$ μW total power. Spectra were acquired using a $50\times$ objective lens with $NA = 0.75$, focussed to a line with dimensions of 20×2 μm with a resulting total excitation intensity of 1.725 kW/cm^2. The Au-sputtered Cu/CuO substrates were functionalized with thiophenol by immersing in a 10 mM ethanolic solution for 30 min, followed by rinsing in pure ethanol and blow-drying with N_2.

Results

Surface analysis

XPS analysis was carried out in order to investigate the oxidation state and chemical bonding of the nanotextured surface. Figure 2(a) shows wide-scan XPS data for the Al K_α photon energy. In order to resolve the Auger electron lines more clearly from the photoelectron contribution, narrow spectral range XPS measurements were conducted at 100 eV higher photon energies.

The high-resolution Cu 2p spectrum is shown in Fig. 2(b), where the Cu $2p_{3/2}$ peak lies at about 933 eV with a shake-up satellite, characteristic of CuO, having around 9 eV higher binding energy than the value observed for the main peak. The peak at 953 eV is attributable to Cu $2p_{1/2}$. The gap between these two energy levels is about 20 eV which is strongly indicative of CuO [21]. High resolution O 1s spectra are shown in Fig. 2(c) with a feature at around 529.3 eV characteristic of a metal-bonded oxygen in CuO.

A broad peak at 531.1 eV was also observed. It's nature was elucidated by measuring the photoelectron spectrum with a significantly lower photon energy of 745 eV. The smaller kinetic energy reduces the energy that the X-ray photons can impart to the electrons, so only the photoelectrons generated relatively close to the surface can escape from the material and be detected. There-

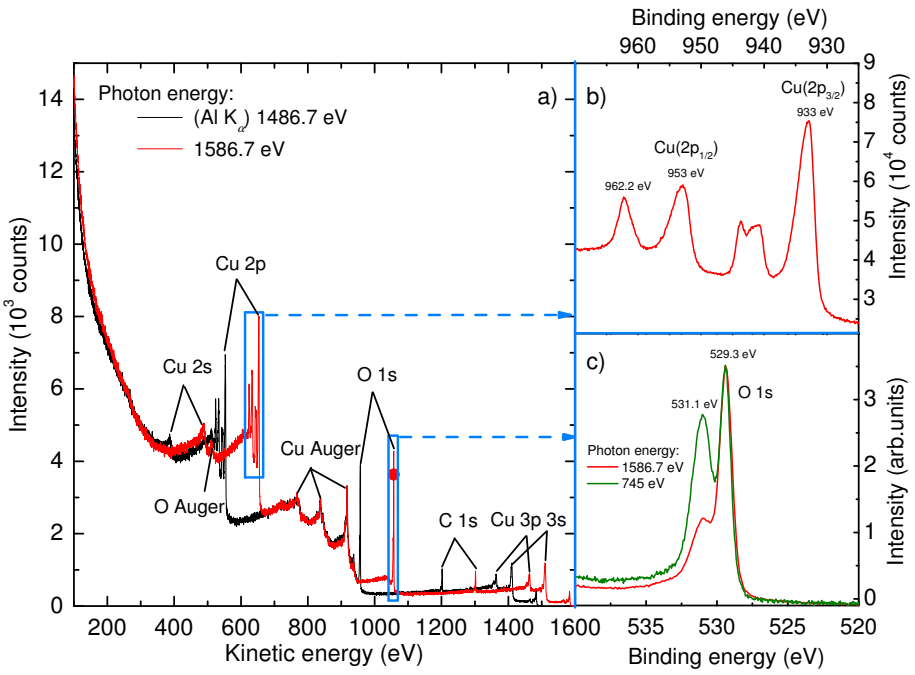

Fig. 2 XPS spectra of chemically-nanostructured Cu layers. (a) Wide-scan photoelectron kinetic energy spectra acquired at different X-ray photon energies. Cu and O Auger electron contributions can be clearly distinguished. (b) High-resolution XPS binding energy spectrum of Cu 2p, characteristic of CuO. (c) High-resolution O 1s spectra, taken at different X-ray photon energies. The increase of the 531.1 eV peak contribution in the lower photon energy spectrum is indicative of a surface-adsorbed oxygen layer.

fore, lower energy XPS spectra are comparatively more sensitive to the surface bound atom contributions. When less energetic X-ray photons are used, the aforementioned 531.1 eV peak in the O 1*s* spectrum increases in relative intensity. This shows that the material which gives rise to this component is physically overlaying the material that gives rise to the lower binding energy peak. Together with the narrow FWHM of O 1*s*, this strongly suggests, that the satellite spectral line can be assigned to adventitious oxygen. Taken in combination, the structure of the Cu $2p_{1/2}$ and O 1*s* spectral lines points towards a chemically uniform CuO coating, with no noticeable trace of Cu_2O and no distribution of environments within the sampling depth of the detected photoelectrons.

A spectral line, indicative of a C 1*s* transition can also be observed at 284.8 eV. The lineshape of this peak (not shown here) points to a surface layer of adsorbed adventitious carbon. This high sensitivity synchrotron XPS analysis proves that "black copper" is composed of CuO. Previous studies have indicated a minor presence of Cu_2O by XPS and Raman surface analysis[17]. This could be explained by the high photosensitivity of CuO and its photo-reduction to Cu_2O as observed in photo-electrochemical cell investigations[18].

Black CuO as SERS substrate

In order to obtain a plasmonic field enchantment for SERS measurements the semiconducting black CuO was coated with Au layers of thicknesses ranging from 25 to 150 nm by magnetron sputtering. These thicknesses correspond to coatings on a flat substrate and were thinner on a black copper surface which has about 200$^\times$ larger surface area. SEM investigation showed that the average thickness of uncoated CuO flakes was $d_0 \approx 30$ nm, increasing to $d_0 \approx 65$ nm after coating with a 150 nm Au layer (Fig. 1). The CuO flakes were Au coated in an isotropic and continuous fashion, as the overall surface structure was preserved. These coated nanoflakes form a complex metallic 3D scaffold with numerous interconnections, nanogaps and crevices which are conducive for plasmonic hot-spot formation, while having an overall structure that is sparse enough to allow for easy diffusion of the analyte molecules to reach areas of strong field enhancement. At higher Au layer thicknesses, nano-rough features formed on the Au coated surface and their footprint and variability escalated as the gold layer thickness increased from 25 to 150 nm.

Figure 3 shows the IR reflectivity of black Cu in the range where SEIRAS is usually measured using FTIR spectrometry. The featureless spectrum with close to linear change in reflectance of the substrate is favorable for molecular fingerprinting by SEIRAS measurements, based on the generally complicated IR spectra of common analytes. In addition, a larger surface area is beneficial for increasing the overall sample absorption.

Thiophenol, which forms a self-assembled monolayer on Au, was used for SERS measurements due to its good stability and capability to benchmark against other Au (or Ag) coated substrates. Thiophenol SERS measurements on substrates with varying Au layer thicknesses are shown in Fig. 4. Strongly pronounced spectral lines characteristic of thiophenol are evident and well resolved. The SERS intensity obtained using these Au-coated black CuO substrates is comparable to the signal levels reported for other high-sensitivity SERS substrates, such as b-Si[22] and ripples

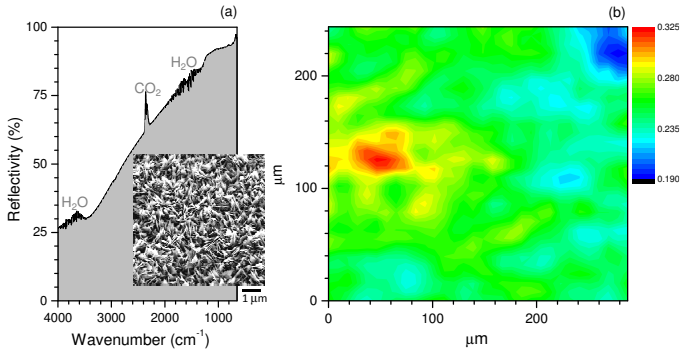

Fig. 3 (a) Reflectivity of black CuO measured by FTIR; spectral regions with artefacts due to CO_2 and H_2O absorption bands are labelled. Reflectivity was normalized to a Au mirror of $R \equiv 1$. Inset shows an SEM image of the sample. (b) FTIR map of reflectivity over an extended area measured with 6.25 μm spatial resolution.

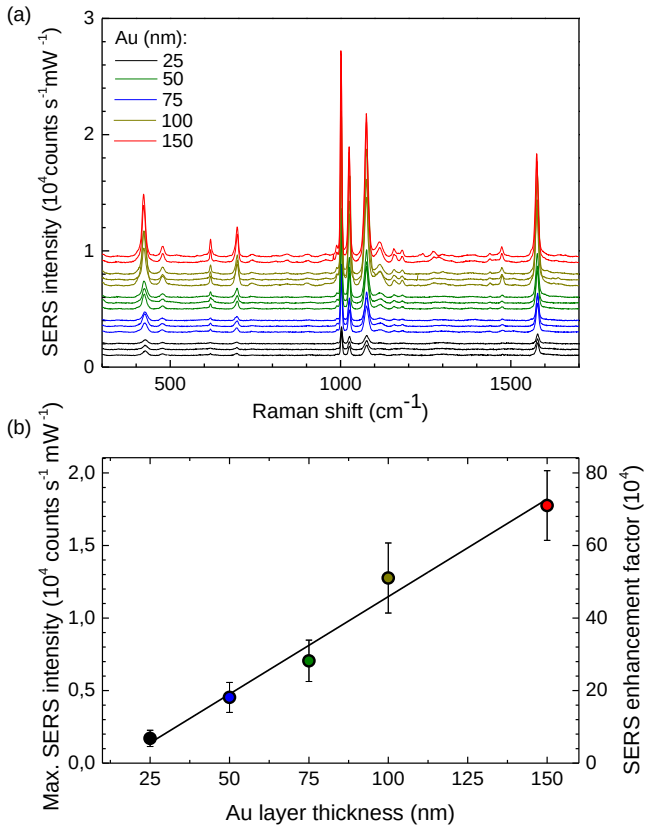

Fig. 4 (a) SERS of thiophenol for different thicknesses of Au coating. Excitation wavelength was 785 nm and SERS intensity was normalised by the excitation power. (b) SERS intensity of the 1001 cm^{-1} thiophenol peak as well as the estimated SERS enhancement factors plotted against Au thickness.

laser inscribed on sapphire[6,8]. However, it is important to note that the preparation of black CuO does not require vacuum or serial laser scanning and is therefore a much faster and less expensive method of surface nanotexturing for large area > 10 cm^2 substrates. In order to evaluate the attainable SERS enhancement factor, meaning the increase in signal strength per molecule, a self-assembled thiophenol monolayer overlaying the Au coated CuO surface was assumed, with molecule coverage characteristics taken from the literature[23]. When weighted against signal per molecule of bulk Raman of thiophenol in solution average enhancement factors up to $7.1 \cdot 10^5$ are estimated. Therefore, simple wet chemical etching can yield large area SERS substrates with enhancement factors close to values reported to enable single molecule detection[24,25].

The SERS enhancement factor, hence, the signal strength is dependent on the thickness of the Au-coating, as illustrated in Fig. 4 (b), where the sensitivity increases linearly with Au thickness. This is attributable to increased nano-roughness and randomization of the surface Au layer, which increases the probability of geometries that support plasmon hot-spots, as has been shown for randomized Au nano-brick arrays[26]. A similar result is observed on black-Si, where a 300 nm Au coating produced the strongest SERS signal[22]. It is noteworthy that the propensity for forming nano-granular films during evaporation and sputtering is dependent on both substrate and coating materials. For sapphire, the nano-roughness of Au was larger than that on a cover glass[19]. Au films directly sputtered onto sapphire can be used for SERS due to the spontaneous formation of nano-rough surfaces[27].

Discussion

The exposure of black surfaces to laser energy leads to localised heating and contamination by adventitious carbon. This is particularly relevant when black CuO is used for SERS, where tightly focused laser beams are applied. In this section, the effects of carbon contamination and laser heating on SERS and SEIRAS measurements are discussed.

Adventitious carbon is often present on SERS substrates and contributes to a broad signal in the range from 1000 - 1700 cm^{-1}, with prominent features at 1360 (D-band) and 1580 cm^{-1} (G-band)[28], and sp^1 CC linear chains at 2100 cm^{-1} assigned to polyyne with alternating single and triple bonds[29,30]. Spectral integration over many measurement points with correspondingly short exposures has been shown to increase the signal-to-noise ratio of the analyte versus adventitious carbon[28]. At smaller wavenumbers the background is dominated by a Rayleigh scattering contribution, shown to be stronger for thicker Au films and recognisable as an augmented SERS intensity baseline. Since plasmon scattering losses are reduced when the thickness of Au approaches the mean free path length of electrons at ~ 40 nm, the stronger SERS intensity signifies a larger contribution of scattering as compared to the absorption losses in the total extinction[31].

In the case of Au coated black CuO on Cu it is possible to realise a C-free surface using electrochemical oxidation of C at -0.5 V (standard hydrogen electrode) or -0.7 V (Ag/AgCl) at pH 13, i.e., in a 0.1 M KOH solution due to CuO being innately compatible with alkaline chemistry. Carbon can be removed from Au surface by means of a short anodic polarisation in the oxygen evolution region, i.e. at $E > 1.8$ V (reversible hydrogen electrode) in a neutral or alkaline medium. Use of acidic solutions is not favourable in this case[32], as the underlying CuO could dissolve chemically through the pores in the deposited Au shell. Under such polarisation, the Au surface is covered by Au_2O_3[19], hence,

should be carbon-free.

Thermal effects are important for adsorption and desorption of ionic and molecular species in SERS and SEIRAS measurements, and sensors in general. The potential of the sensor surface (controlled by local pH or external bias) determines the ratio between free and occupied space on the surface and the balance between the rates of adsorption and desorption in accordance with Nernst equation for potential, given by:

$$E = E^0_{ad} \pm \frac{RT}{F} \ln \frac{c_{ad}}{c_\infty - c_{ad}}, \quad (1)$$

where c_{ad} stands for the surface concentration of adsorbed species in mol·cm^{-2}, c_∞ is the surface concentration of the adsorbate at maximum surface coverage $\Theta = 1.0$, E^0_{ad} is the standard potential of the adsorption process when $c_{ad}/(c_\infty - c_{ad}) = 1$, $R = 8.314$ J·mol^{-1}·K^{-1} is the gas constant, T is the absolute temperature, and $F = 9.6485 \times 10^4$ C·mol^{-1} is the Faraday constant ($RT/F \simeq 25$ mV at normal conditions 20 °C). Consequently, a potential change of ~ 58 mV would cause a tenfold change in the concentration of the surface adsorbate. Given this sensitivity, it is notable that under normal conditions $kT \simeq 26$ meV (or 26 mV in terms of voltage) a small variation of temperature, concentration, or electrical potential in the vicinity of a hot-spot can dramatically affect the nano-sensor response, whether it be SERS or a photonic crystal[33]. Indeed it has been shown that these effects contribute to strong temporal fluctuations in the SERS response[34].

A change of local temperature at the hot spots where SERS is the most intense affects the local concentration of adsorbed species (this is equivalent to a change in surface potential). The Nernst equation defines a Langmuirian behavior of SERS intensity on concentration for the same pattern of hot spots[35]. Moreover, heat is localised on the nanoscale and can initiate chemical reactions[36], which in turn have a strong temperature dependence via the Arrhenius rate equation $k \propto \exp(E_a/(kT))$, where E_a is the activation energy of the process (e.g. a chemical reaction) and k is the Boltzmann constant. In addition, a temperature increase causes a local change in the liquid or gas convection and surface tension, which can dramatically affect mass transport in the vicinity of SERS hot spots[37] as well as the kinetics of chemical reactions. Also, a surface reshaping of gold nanoparticles at ~ 100 °C occurs and can also be responsible for altering light localisation at hot-spots[38].

In view of the discussion above, searching for SERS substrates which have high thermal conductivity such as diamond, sapphire, or metals could prove to be an effective strategy for developing SERS as an *analytical* technique[39]. Analyte trapping at hot spots via the light intensity gradient force - nano-tweezers - has been shown to be the working principle of femto-pico molar detectors based on the lasing wavelength shift in nano-slot lasers[40,41] and had trapping times determined by the diffusion mechanism of adsorption/desorption rule Eqn. 1. Thermal diffusivity and local temperature at the nanoscale should be better understood for the advancement of SERS into practical biomedical applications.

Conclusions

It has been determined by XPS that cupric Cu(II) oxide CuO is formed on black Cu without cuprous Cu(I) Cu_2O during wet etching. The nano-textured surfaces of CuO have a significantly larger surface area which can be conformally coated by sputtering Au. These surfaces are excellent SERS substrates due to the large surface area on which hot-spots may give rise to electromagnetic field enhancement. The SERS intensity counts for a self-assembled monolayer of thiophenol reached $\sim 10^4$ counts/s/mW. Furthermore, such SERS substrates can be electrically biased since they are formed on a conductive Cu foil. Flexible and foldable CuO-on-Cu substrates could be incorporated into flow cells, used for SERS, or in typical large surface area applications for catalysis, fuel cells, supercapacitors, hydrogen generation and storage[42–44].

Acknowledgments

JM acknowledges support by JSPS KAKENHI Grant Number 25420752. SJ is grateful for partial support via Australian Research Council Discovery Project 130101205 and a research visit supported by Tokyo Institute of Technology and the JSPS Top Global University project.

References

1 A. H. Broderick, A. S. Breitbach, R. Frei, H. E. Blackwell and D. M. Lynn, *Adv. Health. Mat.*, 2013, **2**, 993 – 1000.
2 M. V. Graham and N. C. Cady, *Coatings*, 2014, **4**, 37–59.
3 E. P. Ivanova, J. Hasan, H. K. Webb, G. Gervinskas, S. Juodkazis, V. K. Truong, A. H. F. Wu, R. N. Lamb, V. Baulin, G. S. Watson, J. A. Watson, D. E. Mainwaring and R. J. Crawford, *Nature Commun.*, 2013, **4**, 2838.
4 G. Gervinskas, G. Seniutinas, J. S. Hartley, S. Kandasamy, P. R. Stoddart and S. Juodkazis, *Annalen der Physik*, 2013, **525**, 907 – 914.
5 A. Žukauskas, M. Malinauskas, A. Kadys, G. Gervinskas, G. Seniutinas, S. Kandasamy and S. Juodkazis, *Optics Express*, 2013, **21**, 6901–6909.
6 R. Buividas, P. R. Stoddart and S. Juodkazis, *Annalen der Physik*, 2012, **524**, L5 – L10.
7 S. Jayawardhana, L. Rosa, R. Buividas, P. R. Stoddart and S. Juodkazis, *Photonic Sensors*, 2012, **2**, 283–288.
8 A. Chou, E. Jaatinen, R. Buividas, G. Seniutinas, S. Juodkazis, E. L. Izake and P. M. Fredericks, *Nanoscale*, 2012, **4**, 7419 – 7424.
9 Y. Nishijima, Y. Adachi, L. Rosa and S. Juodkazis, *Opt. Mat. Express*, 2013, **3**, 968–976.
10 R. Adato, A. A. Yanik, J. J. Amsden, D. L. Kaplan, F. G. Omenetto, M. K. Hong, S. Erramilli and H. Altug, *PNAS*, 2009, **106**, 19227 – 19232.
11 P. Richharia, *J. Mater. Sci.*, 1989, **24**, 4034 – 4036.
12 O. T. Inal and A. Schrer, *J. Mater. Sci.*, 1986, **21**, 739 – 736.
13 Y. Zhang, L. Su, D. Manuzzi, H. V. E. de los Monteros, W. Jia, D. Huo, C. Hou and Y. Lei, *Biosens. Bioelectron.*, 2012, **31**, 426 – 432.
14 Y. Zhang, Y. Liu, L. Su, Z. Zhang, D. Huo, C. Hou and Y. Lei,

Sensors and Actuators B, 2014, **191**, 86–93.

15 X.-M. Miao, R. Yuan, Y.-Q. Chai, Y.-T. Shi and Y.-Y. Yuan, *J. Electroanalyt. Chem.*, 2008, **612**, 157–163.

16 M.-J. Song, S. W. Hwang and D. Whang, *Talanta*, 2010, **80**, 1648–1652.

17 J. Juodkazytė, B. Šebeka, I. Savickaja, A. Jagminas, V. Jasulaitienė, A. Selskis, J. Kovger and P. Mack, *Electrochimica Acta*, 2014, **137**, 363 – 371.

18 J. Juodkazytė, B. Šebeka, I. Savickaja, A. Selskis, V. Jasulaitienė and P. Kalinauskas, *Electrochimica Acta*, 2013, **98**, 109 – 115.

19 R. Buividas, N. Fahim, J. Juodkazytė and S. Juodkazis, *Appl. Phys. A*, 2013, **14**, 169–175.

20 G. Seniutinas, G. Gervinskas, R. Verma, B. D. Gupta, F. Lapierre, P. R. Stoddart, F. Clark, S. L. McArthur and S. Juodkazis, *Optics Express*, 2015, **23**, 6763 – 6772.

21 P. Riclaharia, K. Chopra and M. Bhatnagar, *Solar Energy Materials*, 1991, **23**, 93–109.

22 G. Gervinskas, G. Seniutinas, J. S. Hartley, S. Kandasamy, P. R. Stoddart, N. F. Fahim and S. Juodkazis, *Annalen der Physik*, 2013, **525**, 907–914.

23 L.-J. Wan, M. Terashima, H. Noda and M. Osawa, *J. Phys. Chem. B*, 2000, **104**, 3563 – 3569.

24 W.-H. Park and Z. H. Kim, *Nano Lett.*, 2010, **10**, 4040 – 4048.

25 P. G. Etchegoin and E. C. L. Ru, *Phys. Chem. Chem. Phys.*, 2008, **10**, 6079 – 6089.

26 Y. Nishijima, J. B. Khurgin, L. Rosa, H. Fujiwara and S. Juodkazis, *Opt. Express*, 2013, **21**, 13502–13514.

27 A. Chou, B. Radi, E. Jaatinen, S. Juodkazis and P. Fredericks, *Analyst*, 2014, **139**, 1960–1966.

28 T. S. B.-S. Yeo, W. Zhang and R. Zenobi, *Appl. Spectrosc.*, 2008, **62**, 708 – 713.

29 C. Casari, A. L. Bassi, L. Ravagnan, F. Siviero, C. Lenardi, E. Barborini, P. Piseri, P. Milani and C. Bottani, *Carbon*, 2004, **42**, 1103 – 1106.

30 A. C. Ferrari and J. Robertson, *Phil. Trans. R. Soc. Lond. A*, 2004, **362**, 2477 – 2512.

31 Y. Nishijima, Y. Hashimoto, L. Rosa, J. B. Khurgin and S. Juodkazis, *Appl. Phys. A*, 2014, **117**, 647–650.

32 K. G. Gallagher and T. F. Fuller, *Phys.Chem.Chem.Phys.*, 2009, **11**, 11557 – 11567.

33 K. Watanabe, Y. Kishi, S. Hachuda, T. Watanabe, M. Sakemoto, Y. Nishijima and T. Baba, *Appl. Phys. Lett.*, 2015, **106**, 021106.

34 S. Šašoć, T. Itoh and Y. Ozaki, *J. Raman Spectr.*, 2005, **36**, 593 – 599.

35 Y. Yokota, K. Ueno, S. Juodkazis, V. Mizeikis, N. Murazawa, H. Misawa, H. Kasa, K. Kintaka and J. Nishii, *J. Photochem. Photobiol. A*, 2009, **207**, 126 – 134.

36 K. Ueno, S. Juodkazis, T. Shibuya, V. Mizeikis, Y. Yokota and H. Misawa, *J. Phys. Chem. C*, 2009, **113**, 11720–11724.

37 O. A. Louchev, S. Juodkazis, N. Murazawa, S. Wada and H. Misawa, *Opt. Express*, 2008, **16**, 5673–5680.

38 A. Plech, R. Cerna, V. Kotaidis, F. Hudert, A. Bartels and T. Dekorsy, *Nano Lett.*, 2007, **7**, 1026 – 1031.

39 R. Buividas, N. Dzingelevicius, R. Kubiliūtė, P. Stoddart, V. K. Truong, E. Ivanova and S. Juodkazis, *J. Biophot.*, 2015), **8**, 567 – 574.

40 S. Kita, S. Hachuda, K. Nozaki and T. Baba, *Appl. Phys. Lett.*, 2010, **97**, 161108.

41 D. Takahashi, S. Hachuda, T. Watanabe, Y. Nishijima and T. Baba, *Appl. Phys. Lett.*, 2015, **106**, 131112.

42 K. Juodkazis, J. Juodkazytė, B. Šebeka and S. Juodkazis, *Appl. Surf. Sci.*, 2014, **290**, 13–17.

43 K. Juodkazis, J. Juodkazytė, A. Grigucevičienė and S. Juodkazis, *Appl. Surf. Sci.*, 2011, **258**, 743–747.

44 K. Juodkazis, J. Juodkazytė, P. Kalinauskas, E. Jelmakas and S. Juodkazis, *Opt. Express: energy express*, 2010, **18**, A147–A160.